Actinic photoemission spectroscopy of litho materials using a table-top ultrafast EUV source

Dhirendra P. Singh[1], Kevin M. Dorney[1], Fabian Holzmeier[1], Esben W. Larsen[1], Laura Galleni[1,2], Charles Mokhtarzadeh[3], Michiel J. van Setten[1], Thierry Conard[1], John S. Petersen[1], and Paul A. W. van der Heide[1]

[1]Imec, Kapeldreef 75, 3001 Leuven, Belgium
[2]Department of Chemistry, KU Leuven, Celestijnenlaan 200F, 3001 Leuven, Belgium
[3]Intel Corporation, 2501 NE Century Blvd., Hillsboro, Oregon, USA 97124

ABSTRACT

Extreme ultraviolet (EUV) lithography (92 eV) has recently entered logic and memory high-volume manufacturing to ensure the continuation of Moore's Law into advanced technology nodes (sub 5 nm). In parallel to advancements in the lithographic system, the development of suitable photoresists plays an equally important role in pushing the boundaries of EUV lithography. Fundamental work on well-established chemically amplified resists (CAR) for EUV as well as the upcoming resists based on metal-organic materials have indicated that the lithographic mechanism is largely governed by electron mediated chemistry. In a simplified model, the electrons emitted upon ionization of the material generate further secondary electrons, which interact with the resist components and induce a solubility switch driven by electron and radiation chemistry. To develop a better performing resist, it is of utmost importance to understand the photoelectron kinetic energy spectrum, secondary electrons and their generation efficiency, and the electron mean free path in the photoemission process. In this work, we use photoemission spectroscopy with a table-top, coherent, 92 eV photon source to shed light on the chemistry driven by photon exposure. The valence band photoelectron spectrum (PES) of an environmentally stable chemically amplified photoresist (ESCAP), as well as a model material for an open-source metal oxide (OSMO) resist were measured using our tabletop EUV photoemission setup. We report the evolution of the PES as a function of exposure dose; capturing chemical changes.

Keywords: extreme ultraviolet (EUV), extreme ultraviolet lithography, chemically amplified and metal-oxide photoresist, secondary electrons, photoelectron spectroscopy, electron-induced chemistry

1. INTRODUCTION

Photoelectron spectroscopy is a technique based on the photoelectric effect [1], a phenomenon in which a photon with higher energy than the work function of a material removes electrons from the materials. Depending on the photon energy used, electrons can be removed from the valence band, a semi-core level, or a core level. Thus, the photoelectron spectrum is composed of emission peaks from these levels and a "tail" of the secondary electrons. This secondary electron "tail" is the result of (in)elastic electron scattering events that produce a large amount (relative to the direct photoelectrons) of low-energy electrons. The electron mean free path for electrons with kinetic energy (E_{kin}) of 10-150 eV in solids is relatively short [2, 3], making it a surface-sensitive technique. However, for lower energy electrons, E_{kin}< 5eV, the mean free path is larger making these electrons slightly sensitive to the bulk as well [3].

Upon photon exposure in photoresist material, the photoemission process occurs, the primary electrons undergo inelastic scattering giving rise to multiple slow secondary electrons. These secondary electrons can initiate and drive chemical transformation within photoresist. From the PES, we can get insight into these primary and secondary electrons shedding light on which electrons are inducing more significant changes in photoresist. Moreover, EUV photons can also interact with the substrate and underlayer leading to a similar process of electron emission and inelastic scattering, which may possibly alter and affect chemical changes in the resist layer. Hence, gaining a comprehensive understanding of the

Metrology, Inspection, and Process Control XXXVIII, edited by Matthew J. Sendelbach, Nivea G. Schuch, Proc. of SPIE Vol. 12955, 1295504 · © 2024 SPIE
0277-786X · doi: 10.1117/12.3010751

processes triggered by interactions between EUV photons, the photogenerated electrons, and the resist layer or possibly the full resist stack is of utmost importance.

2. EXPERIMENTAL DETAILS

The experimental apparatus setup has been described in detail elsewhere [4, 5]. Briefly, the valence band photoelectron spectrum of an environmentally stable chemically amplified photoresist (ESCAP) and an open-source metal oxide (OSMO) resist were measured using a hemispherical photoelectron analyzer (KREIOS 150, SPECS GmbH) coupled with a laser-driven EUV light source (XUUS4, KMLabs) based on high-harmonic generation (HHG). The HHG process was performed in Helium gas, resulting in a tunable spectrum with a bright, narrowband harmonic at ~92 eV ($\Delta\lambda/\lambda \sim 10^{-2}$) that was used in this work. The 92 eV EUV beam was coupled into the KREIOS spectrometer via a toroidal focusing mirror (f = 40 cm) resulting in a spot size of ~100 x 50 μm^2 (elongated due to a grazing incidence angle of ~30 degrees).

Samples were mounted on a metal plate with a conducting clip to minimize the effects of surface charging and transferred into the analysis chamber (~5 x 10^{-10} mbar) of the KREIOS tool for measurements of the PES. The incident EUV beam power was attenuated using zirconium foils (150 and 300 nm) placed upstream in the beamline to further reduce the effects of surface charging and to ensure that the flux is low enough to reduce the degradation of the photoresist during the first few spectra. The PES was collected with a pass energy of 100 eV and the entrance slit was of the hemispherical analyzer was set to 0.8 mm.

In our tool, the writing speed (EUV exposure) can be controlled from ~10-100 $\mu J/s/cm^2$ (dose of ~1-10 mJ/cm^2 for an energy scan of range 5-100 eV). The valence band PES was measured with an EUV dose of approximately 1-2 mJ/cm^2. Figure 1a shows ten successive spectra measured for ESCAP showing no changes upon exposure. The ten spectra are averaged for better signal-to-noise ratio and the standard deviation is shown in Figure 1b. To capture changes in the photoelectron spectra during exposure, the spectra were collected for several hours leading up to the total EUV dose of approximately 250-300 mJ/cm^2.

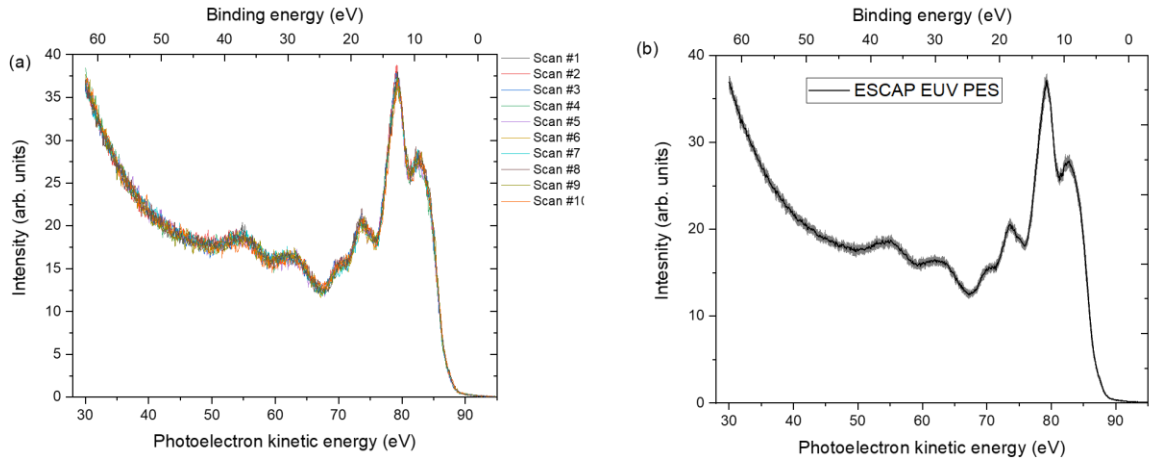

Figure 1. (a) Ten successive EUV photoelectron spectra of ESCAP using 92 eV photons (EUV dose ~1 mJ/cm^2/scan). (b) An average of ten EUV PES with statistical error (gray color).

Photoresist samples were prepared via spincoating of the stock solutions. A modified version of the ESCAP was provided by FujiFilm. The composition of the modified ESCAP material was as follows: a backbone polymer of p-hydroxystyrene (48 mol%) and tert-butyl methacrylate (52 mol%), (4-Methylphenyl) diphenyl sulfonium nonaflate as the photoacid generator (17.3 wt%) (PAG), and trioctylamine as the quencher (7.1 wt%). In all photoresist samples, the thickness of the photoresist was determined by fitting reflectance curves from a commercial spectroscopic ellipsometer (RC2, JA Woollam Company). To achieve high quality fits, blank Si coupons (i.e., with no photoresist) were first measured to determine the thickness of the native SiO_2. The optical constants from these initial fits were then used in the fitting of the ellipsometry data to obtain thickness values of ~30 nm for the ESCAP material.

For OSMO sample preparation 500 mg's of $[(n\text{-}BuSn)_{12}O_{14}(OH)_6][OAc]_2$ was dissolved in 5.00 g's of anhydrous MeOH (0.1 wt % solution). The resulting material was sealed under nitrogen brought out of the glovebox and sonicated for 15 mins to solubilize $[(n\text{-}BuSn)_{12}O_{14}(OH)_6][OAc]_2$. The material was then brought back into the glovebox and filtered over a 0.2 μM filter to remove micro particles into clean room class 100 grade FFP bottle and stored until used. The films of the OSMO material were prepared by spincoating followed by a post application bake to removal any residual solvent in the film. The resulting film thickness was ~ 22 nm, as verified by spectroscopic ellipsometry.

3. RESULTS AND DISCUSSION

In the following, we report the photoemission spectra of ESCAP and OSMO with 92 eV excitation. The EUV exposure-driven changes in the valence band were captured in the photoelectron spectrum of these materials shedding light on decomposition pathways.

3.1 ESCAP photoelectron spectrum

ESCAP is composed of various components and the molecular orbitals from these components form the valence band. In Figure 1 the photoelectron spectrum of ESCAP using 92 eV photons shows the emission from the valence band and semi-core orbitals. As the valence band and semi-core level region of the PES are largely determined by the chemical character of the material (as opposed to the deeper core level which are more atomic in character), EUV-induced chemical changes are expected to manifest most strongly in this region. Tracking changes in this photoelectron energy range thus gives the capability to extract chemical changes resulting from EUV exposure.

To unravel EUV-exposed chemical change, we looked at three different samples, unexposed, a nominal exposure dose of 40 mJ/cm^2, and a high dose of 200 mJ/cm^2 (overexposed). The EUV exposures were done in an external tool, (details of the setup are presented elsewhere [6]) exposing the whole 1x1 cm sample. Figure 2a shows the PES measured using 92 eV photon energy (dose ~2 mJ/cm^2/scan, average of 5 scans). Upon comparison, we observe subtle changes in the intensity of a few peaks and shifts in the peak position. At low exposure dose, the intensity of the peaks does not vary significantly, but a small shift in peak position was observed toward higher electron kinetic energy. However, for the overexposed sample, the intensity of the peaks around 10-15 eV and 35 eV binding energy was reduced with minor shift in the peak position.

To understand the variation observed in the PES collected from two different exposures, the peak assignment was done using the methodology explained in Ref. [7]. The theoretical binding energies were computed with Turbomole 7.2 using single-shot *GW* on top of density functional theory with the BH-LYP hybrid functional and a Gaussian basis set of split valence quality (def2-SVP). The *GW* calculations were performed on each separate component of the ESCAP material embedded in atomic charges and dipole moments, which were obtained from a microelectrostatic calculation using the MESCal code. The spectra of all components, obtained after applying a Gaussian broadening of 0.65 eV, were then summed up after scaling the intensity by the corresponding molar ratio.

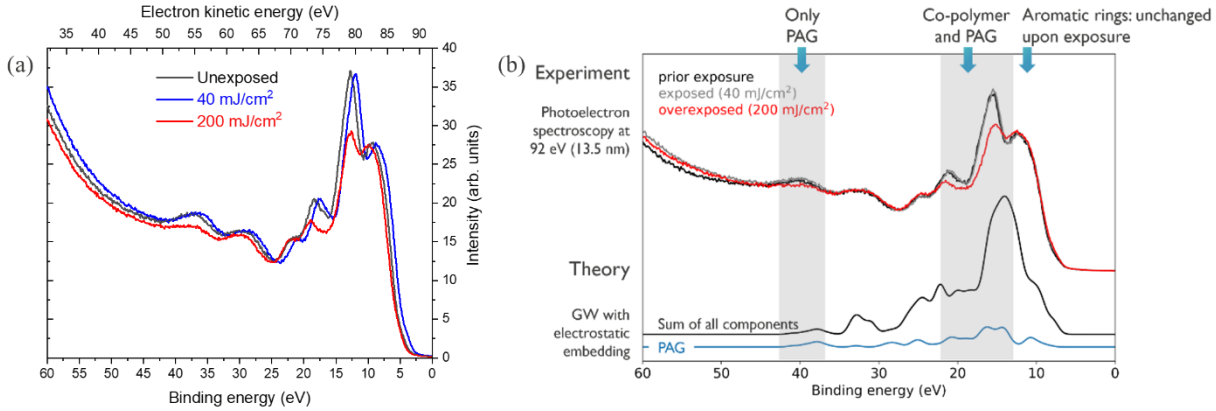

Figure 2. (a) Comparison of unexposed, exposed, and overexposed photoelectron spectrum of ESCAP using 92 eV photons. (b) Simulated PES spectrum and the peak assignment.

Figure 2b shows that the peak at binding energy 35 eV mainly comes from the PAG and peaks between 10-15 eV binding energy originate from the PAG and polymer. A similar assignment was presented by Kostko and co-authors [8] for a CAR model resist. These observations indicate a PAG (possibly polymer too) decomposition upon exposure as expected in these types of resist systems [8].

To capture EUV exposure driven change during the PES measurement itself, a longer duration of measurements was carried out (as mentioned in the experimental section). Figure 3 shows a long-duration EUV PES measurement at 92 eV (dose 2 mJ/cm^2/scan) in the form of a "waterfall" plot of all the collected PES up to the total exposure dose of 300 mJ/cm^2. There is a close similarity between the externally exposed PES figure 2 (overexposed) and long in-situ exposure Figure 3. First, we see the intensity reduction in the peak around 80 eV E_{kin} (Figure 3a), showing similar behavior of PAG and possibly polymer decomposition. Second, we see similar charge dynamics (observed previously in Figure 2a) around dose 50 mJ/cm^2 in figure3b, where we see a shift in the peak positions towards higher $E_{kin.}$ A deeper understanding of this peak position shift will be investigated in future work.

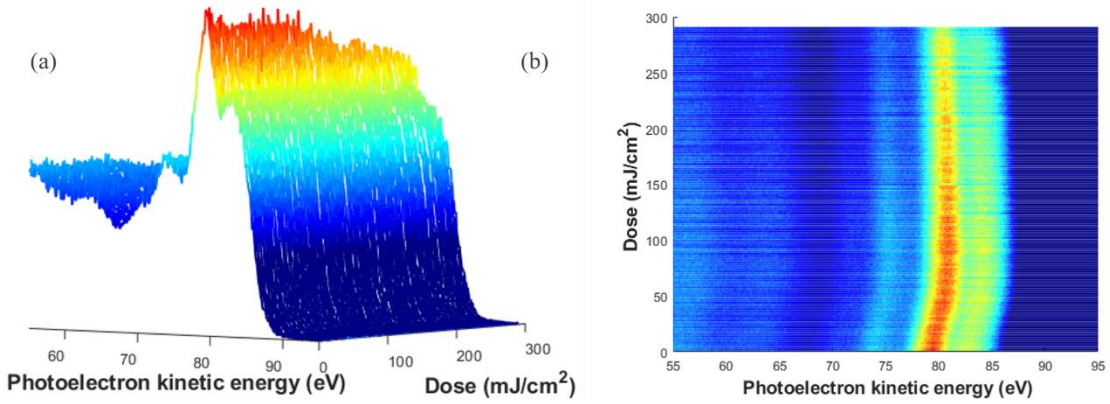

Figure 3. Long exposure EUV photoelectron spectra of ESCAP using 92 eV photon (dose 2 mJ/cm^2/scan). (a) and (b) are different orientations of the view for long exposure EUV PES.

3.2 OSMO photoelectron spectrum

Metal-oxide-based resist with organic ligands show immense potential for EUV lithography owing to their higher absorption cross section at 92 eV as well as higher etch resistance [9]. In this work, we report a PES study on tin-based open-source metal oxide (OSMO) model photoresist. It consists of a tin-oxo cage structure with n-butyl ligands and acetate counter anions [10, 11].

The highest lying molecular orbitals are located mainly around Sn-C bonds, thus removal of an electron (via direct photoionization) would weaken these bonds and butyl cleavage is expected [12]. The photoemission work could unravel the exposure-driven chemical pathways in these resist systems.

Figure 4a presents the EUV PES for OSMO resist, with valence band region in the binding energy range 5-25 eV and a semi-core peak of Sn 4d orbitals at binding energy 28.26 eV. In Figure 4b we present the long-exposure PES as a function of exposure dose.

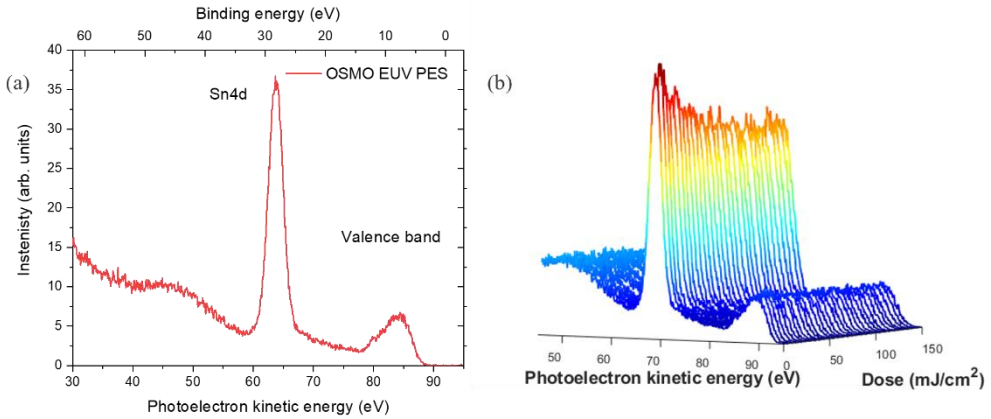

Figure 4. (a) PES of OSMO at 92 eV (dose = 5 mJ/cm^2, 1 scan). (b) PES evolution as a function of dose at 92 eV (dose = 5 mJ/cm^2/scan).

Furthermore, a post-exposure baking (PEB) step was added to the experimental procedure to understand thermal-driven pathways. Baking was done at 180 degree C for 10 mins in vacuum (in the same tool), followed by PES measurement. Figure 5a shows the comparison of unexposed (1 scan, dose = ~5 mJ/cm^2), exposed (dose = ~150 mJ/cm^2), and PEB spectra. At first glance comparing unexposed and exposed spectra, the Sn 4d peak shows a reduction in the intensity along with peak broadening and peak shift upon exposure. As the peak shift is towards higher binding energy, this could indicate the possibility of surface charging due to photoionization process. To further understand the nature of the broadening and shift we need computational work which is beyond the scope of this article.

Moreover, upon baking we observed completely different valence band spectra and a different peak position for the Sn4d peak, a shift towards lower binding energy. Figure 5b shows the PES spectrum after post-exposure bake, the binding energy for Sn4d peak is 26.76 eV, which upon comparison is similar to the Sn4d peak (26.63 eV) for SnO_2 films measured using X-ray photoemission spectroscopy (XPS) [13]. Furthermore, the PEB valence band region shows a similarity to the valence band of SnO_2 film measured at 100 eV photon energy [14]. This comparison of Sn4d peak and valence band region of post exposure bake PES indicates the possible formation of an increased amount of Sn-O-Sn after the bake, which is consistent with the expected mechanism where an insoluble network of linked Sn cages is formed after exposure and PEB.
To further investigate the exposure driven changes, we are planning to use a residual gas analyzer to collect mass spectra during the bake. Moreover, while PES measurements are strong indicators of the expected chemistry, coupling PES measurements with chemical spectroscopies (e.g., FTIR and XPS) will yield increased insights in the exposure mechanism.

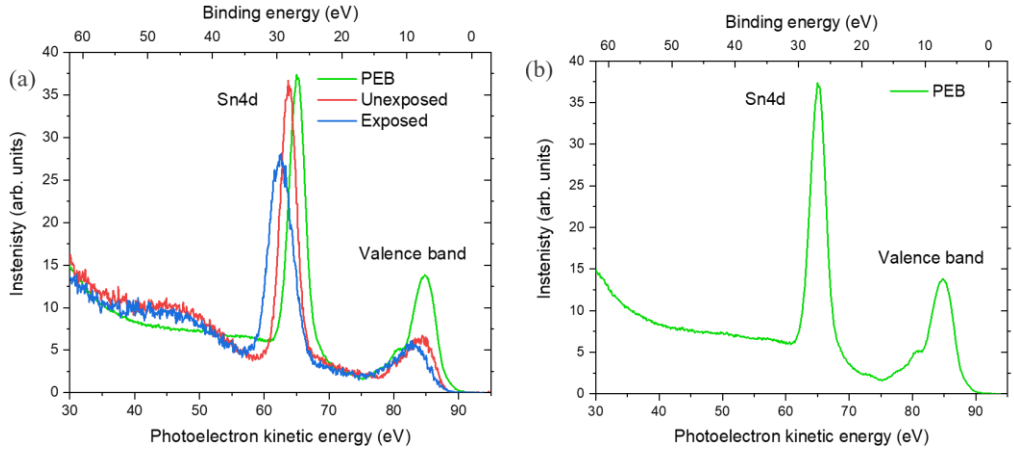

Figure 5. (a) Comparison of OSMO unexposed, exposed, and PEB photoelectron spectra using 92 eV photon energy. (b) Post-exposure bake EUV PES.

4. CONCLUSIONS

EUV photoelectron spectra of two model photoresist systems were investigated to understand the exposure-driven changes. The model CAR (ESCAP) EUV PES were reported for both externally exposed and in-situ exposure. The PES at a lower dose of < 50 mJ/cm^2 essential remains unchanged, only a subtle shift in the peak positions to higher electron kinetic was observed. Further, at higher doses (200-300 mJ/cm^2), we observed the degradation of a peak originating from PAG and possibly polymer.

For the model metal oxide resist (OSMO) EUV PES was reported along with the long in-situ exposure PES measurement. The PES shows a gradual change as a function of dose, a shift and peak broadening were observed of the Sn4d peak. Further, the PEB PES indicated the cleavage of organic ligands leading to condensation of tin-oxo cage and formation of Sn-O-Sn linkages.

ACKNOWLEDGMENTS

D. P. S. and K. M. D. acknowledge funding from the European Union's Horizon 2020 research and innovation program under the Marie Sklodowska-Curie grant agreement No.'s 101032241 (D.P.S.) and 101031245 (K.M.D.). We also gratefully acknowledge FujiFilm for providing the model ESCAP material used in this work. We would also like to thank Roberto Fallica, Ivan Pollentier, and Danilo De Simone for their support and assistance. We would also like to acknowledge James M. Blackwell of Intel for in-depth technical conversations.

REFERENCES

[1] Albert Einstein, "Über einen die Erzeugung und Verwandlung des Lichtes betreffenden heuristischen Gesichtspunkt". Annalen der Physik. Vol. 322 No. 6 (1905) https://doi.org/10.1002/andp.19053220607

[2] Tanuma, S., Powell, C.J., Penn, D.R., "Calculations of electron inelastic mean free paths. ix. data for 41 elemental solids over the 50 eV to 30 keV range". Surf. Interface Anal. 43, 689– 713 (2011)

[3] Olga Yu. Ridzel, Vytautas Astašauskas, Wolfgang S.M. Werner, "Low energy (1–100 eV) electron inelastic mean free path (IMFP) values determined from analysis of secondary electron yields (SEY) in the incident energy range of 0.1–10 keV", Journal of Electron Spectroscopy and Related Phenomena, Volume 241, 146824, (2020) https://doi.org/10.1016/j.elspec.2019.02.003.

[4] F. Holzmeier, K. Dorney, E. W. Larsen, T. Nuytten, D. P. Singh, M. van Setten, P. Vanelderen, C. Bargsten, S. L. Cousin, D. Raymondson, E. Rinard, R. Ward, H. Kapteyn, S. Böttcher, O. Dyachenko, R. Kremzow, M. Wietstruk, G. Pourtois, P. l van der Heide, J. Petersen, "Introduction to imec's AttoLab for ultrafast kinetics of EUV exposure processes and ultra-small pitch lithography," Proc. SPIE 11610, Novel Patterning Technologies 2021, 1161010 (22 February 2021); https://doi.org/10.1117/12.2595038

[5] K. M. Dorney, N. N. Kissoon, F. Holzmeier, E. W. Larsen, D. P. Singh, S. Arvind, S. Santra, R. Fallica, I. Makhotkin, V. Philipsen, S. De Gendt, C. Fleischmann, P. A. W. van der Heide, J. S. Petersen, "Actinic inspection of the EUV optical parameters of lithographic materials with lab-based radiometry and reflectometry," Proc. SPIE 12494, Optical and EUV Nanolithography XXXVI, 1249407 (28 April 2023); https://doi.org/10.1117/12.2658359

[6] I. Pollentier, I. Neira, and R. Gronheid "Assessment of resist outgassing related EUV optics contamination for CAR and non-CAR material chemistries", Proc. SPIE 7972, Advances in Resist Materials and Processing Technology XXVIII, 797208 (15 April 2011); https://doi.org/10.1117/12.881215

[7] L. Galleni, A. Meulemans, F. S. Sajjadian, D. P. Singh, S. Arvind, K. M. Dorney, T. Conard, G. D'Avino, G. Pourtois, D. Escudero, M. J. van Setten, "Peak Broadening in Photoelectron Spectroscopy of Amorphous Polymers: The Leading Role of the Electrostatic Landscape," J. Phys. Chem. Lett. 15(3), 834–839 (2024); https://doi.org/10.1021/acs.jpclett.3c02640

[8] Oleg Kostko, Terry R. McAfee, Patrick P. Naulleau, "Role of resist components in electron emission and capture", International Conference on Extreme Ultraviolet Lithography 2023, 39, (2023); doi:10.1117/12.2687332

[9] Kazuki Kasahara, Hong Xu, Vasiliki Kosma, Jeremy Odent, Emmanuel P. Giannelis, Christopher K. Ober, Recent Progress in EUV Metal Oxide Photoresists, Journal of Photopolymer Science and Technology, Volume 30, Issue 1, Pages 93-97 (2017)
[10] Frederic Banse, F. Ribot, P. Toledano, J. Maquet, and C. Sanchez, "Hydrolysis of Monobutyltin Trialkoxides: Synthesis and Characterizations of $\{(BuSn)_{12}O_{14}(OH)_6\}(OH)_2$", Inorganic Chemistry 34 (25), 6371-6379 (1995) DOI: 10.1021/ic00129a023
[11] Brian Cardineau, Ryan Del Re, Miles Marnell, Hashim Al-Mashat, Michaela Vockenhuber, Yasin Ekinci, Chandra Sarma, Daniel A. Freedman, Robert L. Brainard, "Photolithographic properties of tin-oxo clusters using extreme ultraviolet light (13.5nm)", Microelectronic Engineering, 127, 44-50, ISSN 0167-9317, (2014) https://doi.org/10.1016/j.mee.2014.04.024.
[12] I. Bespalov, Y. Zhang, J. Haitjema, R. M. Tromp, S. J. van der Molen, A. M. Brouwer, J. Jobst, and S. Castellanos, "Key role of very low energy electrons in tin-based molecular resists for extreme ultraviolet nanolithography," ACS Appl. Mater. Interfaces 12, 9881–9889 (2020).
[13] Anil R. Chourasia, Allen E. Hillegas; Analysis of tin and tin oxide by x-ray photoelectron spectroscopy. Surf. Sci. Spectra; 28 (1): 014003 (1 June 2021) https://doi.org/10.1116/6.0000528
[14] Yoshihiro Aiura, Kenichi Ozawa, Izumi Hase, Kyoko Bando, Hiroto Haga, Hirofumi Kawanaka, Akane Samizo, Naoto Kikuchi, and Kazuhiko Mase, "Disappearance of Localized Valence Band Maximum of Ternary Tin Oxide with Pyrochlore Structure, Sn_2Nb_2O," The Journal of Physical Chemistry C 121 (17), 9480-9488 (2017) DOI: 10.1021/acs.jpcc.6b12572